Fibonacci lattices for the evaluation and optimization of map projections

Sergio Baselga

Cartographic Engineering, Geodesy and Photogrammetry Dept., Universitat Politècnica de València, Camino de Vera s/n, 46022 Valencia, Spain. E-mail address: serbamo@cgf.upv.es

ABSTRACT

Latitude-longitude grids are frequently used in geosciences for global numerical modelling although they are remarkably inhomogeneous due to meridian convergence. In contrast, Fibonacci lattices are highly isotropic and homogeneous so that the area represented by each lattice point is virtually the same. In the present paper we show the higher performance of Fibonacci versus latitude-longitude lattices for evaluating distortion coefficients of map projections. In particular, we obtain first a typical distortion for the Lambert Conformal Conic projection with their currently defined parameters and geographic boundaries for Europe that has been adopted as standard by the INSPIRE directive. Further, we optimize the defining parameters of this projection, lower and upper standard parallel latitudes, so that the typical distortion for Europe is reduced a 10% when they are set to 36º and 61.5º, respectively. We also apply the optimization procedure to the determination of the best standard parallels for using this projection in Spain, whose values remained unspecified by the National decree that commanded its official adoption, and obtain optimum values of 37º and 42º and a resulting typical distortion of 828 ppm.

Keywords: Fibonacci lattices; Lambert Conformal Conic projection; standard parallels; optimization.

1. Introduction

The effective evaluation of scalar models for a particular area is an issue frequently encountered in geosciences. The standard approach is to use regular latitude-longitude lattices, which are conceptually simple and generally easy to implement in any software. They suffer, however, from fundamental problems especially associated with the meridian convergence, which often make them ineffective for the evaluation of the model in the geographic area under study.

In the last decades, some alternatives to latitude-longitude lattices have been proposed for global numerical modelling, which have some desirable properties such as higher geometrical regularity and isotropic spatial resolution as well as ease of parallelization (Purser 1999). They generally require a lower number of lattice points than standard latitude-longitude lattices to obtain results of the same quality. Among them, Fibonacci lattices have emerged as powerful tools to enhance numerical effectiveness due to their virtual uniformity and isotropic resolution (Swinbank and Purser, 2006).

While the regular hexagonal lattice provides optimal sampling for the plane (Conway and Sloane, 1998), it is impossible to arrange regularly more than 20 points on the sphere let alone on the ellipsoid. The usual latitude-longitude lattice is highly inhomogeneous and far from the desired situation where every point represents almost the same area, which can be virtually obtained with the use of a Fibonacci lattice, a mathematical idealization of natural patterns with optimal packing. González (2010) takes advantage of this feature and applies Fibonacci lattices to the problem of area determination by means of point counting, obtaining results with at least 40% error reduction when compared to the use of latitude-longitude lattices. Other applications of Fibonacci lattices can be found in disparate fields as shallow water modelling, climate models and three-dimensional numerical weather prediction (Swinbank and Purser, 2006) including tornado outbreak prediction (Sparrow and Mercer, 2016), air traffic networks (Monechi *et al.* 2015), electron paramagnetic resonance (Crăciun, 2014) and approximation of spherical integrals for image sampling (Marques *et al.* 2013).

In the present paper we propose to apply Fibonacci lattices first as a tool to evaluate map projection distortions and then to optimize their defining parameters so that the resulting map projection has minimum distortion for a particular area of use. More specifically, starting from Airy (1861) and Jordan (1896)'s measures of distortion, we will define an optimization function based on the square mean deviation from unity of the scale distortion coefficient of a conformal map projection over a representative Fibonacci lattice of the area under study and compute its optimum. Since Conic Map projections are suitable for mid-latitude regions with predominant East-West extension (Snyder, 1987; Savric and Jenny, 2016), they have often been required or recommended by national mapping agencies or international consortiums. In particular, the Lambert Conformal Conic projection was proposed, first, by EuroGeographics, the consortium of European national mapping, cadastral and land registry authorities (Annoni *et al.*, 2003) for conformal representations of Europe, and then adopted by INSPIRE D2.8.I.1 (2014), the European Commission directive for spatial information, as the standard for conformal mapping in Europe. We want now to evaluate the distortions this projection introduces, first, and then investigate whether the definition of other standard parallels than the two recommended by EuroGeographics and then adopted by INSPIRE, produces significantly better results. As an additional example, we will also apply our methods to the particular case of Spain, where the Lambert Conformal Conic projection has been officially adopted for land representation at mapping scales of 1:500.000 or lower (Gobierno del Estado Español, 2007). This decree does not fix, however, the standard parallel latitudes to be used, so we will compute the ones that minimize the resulting distortions by means of our method based on Fibonacci lattices.

2. Methods

2.1. Latitude-longitude lattices

For a given geographic domain, a latitude-longitude lattice is easily constructed after the definition of a grid step δ, so that points are generated for all pairs that can be formed with (φ_{min}, $\varphi_{min} + \delta$, $\varphi_{min} + 2\delta$, ...) (all latitudes lower than the maximum possible latitude) and (λ_{min}, $\lambda_{min} + \delta$, $\lambda_{min} + 2\delta$, ...) (all longitudes lower than the maximum possible longitude). Due to the meridian convergence the distribution of points is denser in polar areas, which makes the lattice remarkably inhomogeneous.

When we use latitude-longitude lattices we normally need a considerably large number of sampling points in the area (small step size δ) to obtain a stable value that does not depend significantly on the number of sampling points. Even then the value may oscillate a bit. We can improve the performance of latitude-longitude lattices by using a weighting function so that the abundance of points at higher latitudes is compensated by a lower weight in the computation. Following González (2010) in order to compensate for higher density at higher latitudes we must use for every lattice point *i* the weight function

$$w_i = \cos\varphi_i \tag{1}$$

2.2. Fibonacci lattices

Contrary to latitude-longitude lattices, a Fibonacci lattice has the property of regular isotropic distribution. It bears its name from Leonardo Pisano, alias Fibonacci, a medieval mathematician who discovered the sequence 0, 1, 1, 2, 3, 5, 8, 13, 21... in which every number (starting from the third) is the sum of the previous two. This series, initially developed by Fibonacci to account for the population of rabbit breeding in the different generations, appears in many biological systems (such as branching and arrangement of leaves in plants and trees, petal flowering, beehives, etc.) as well as in chemical composition of materials, music theory and other apparently detached areas such as economic theory (see e.g. Koshy, 2001). As the series progresses to infinity, the ratio between consecutive numbers, F_i and F_{i+1}, approaches the so-called golden ratio Φ

$$\lim_{i\to\infty} \frac{F_{i+1}}{F_i} = \Phi \qquad (2)$$

This golden ratio is the number whose inverse is the number itself minus one

$$\Phi = 1 + \frac{1}{\Phi} = \frac{1+\sqrt{5}}{2} \approx 1.61803399 \qquad (3)$$

The Fibonacci lattice is generated by a spiral with evenly spaced points, being the longitudinal turn between consecutive points defined by $360^{\circ}\Phi^{-1} \approx 222.5^{\circ}$ or by its complement to 360º, i.e. $360^{\circ}(1-\Phi^{-1}) = 360^{\circ}\Phi^{-2} \approx 137.5^{\circ}$. Following González (2010) we generate a Fibonacci lattice with longitudinal turns between consecutive points of $360^{\circ}\Phi^{-1}$, if, given a natural number N, we compute the set of geographic coordinates for points $i = -N, -N+1, \ldots, 0, N-1, N$ as

$$\begin{aligned} \varphi_i &= \arcsin\left(\frac{2i}{2N+1}\right) \times \frac{180^{\circ}}{\pi} \qquad i = -N, -N+1, \ldots, 0, N-1, N \\ \lambda_i &= 360^{\circ}\,\Phi^{-1} i = 360^{\circ} \times \mathrm{mod}(i, \Phi) / \Phi \end{aligned} \qquad (4)$$

The function $\mathrm{mod}(i,\Phi)$ returns the remainder of the division of i by Φ, eliminating thus the unnecessary turns of the spiral (i.e. additive values of 360º for each spiral turn). The geographic coordinates φ_i, λ_i that are obtained by means of Eq. (4) for every point i of the lattice are given in degrees. This results in $2N+1$ total points for the lattice, being each of them located in a different latitude, which provides a much more homogeneous sampling than the case of the latitude-longitude lattice. Just for the purpose of illustration we depict in Fig. 1 the results of a latitude-longitude lattice over a sphere with 180 points ($\delta = 20^{\circ}$) and in Fig. 2 the results of a Fibonacci lattice over a sphere with 179 points (Fibonacci lattices always have an odd number of points). While in Fig. 1 a high point density in polar areas contrasts with a quite sparse distribution of points near the equator, in Fig. 2 we have a much more uniform point density.

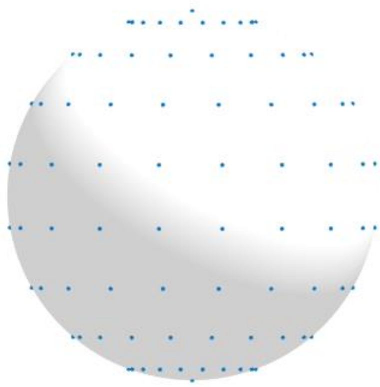

Fig. 1. Latitude-longitude lattice (180 points)

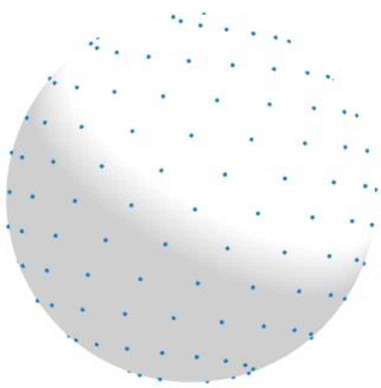

Fig. 2. Fibonacci lattice (179 points)

2.3. Distortion measures

When we want to project a spherical surface onto a plane, distortions of several type will inevitably occur due to the fact that the sphere has a finite radius of curvature whereas the plane has an infinite one. This is also the case when the source reference surface is an ellipsoid. Distortions in the map projection are normally classified into linear distortions, areal distortions and angular distortions (Snyder, 1987). Some projections have been devised to avoid a particular type of distortion (e.g. so-called conformal projections avoid angular distortions and so-called equal-area projections avoid areal distortions), others have been designed for a compromise of approximate preservation of all properties (they yield tolerable errors in all linear, angular and areal measures), but none of them is completely free from distortions, so that instead of a perfect map projection for universal use we can find many different map projections each of them devised for a particular purpose and geographic area (Snyder, 1987; Canters and Decleir, 1989).

Conformal projections are currently used for producing official cartography such as national topographic maps. They preserve angles but suffer from different distortions in length and area. For a pair of infinitesimally close points *i* and *j*, we can define the linear distortion coefficient k_1 as the ratio of the projected distance ds' to the original distance on the sphere or ellipsoid surface ds and obtain, after some derivations using differential geometry (Baselga, 2014), that

$$k_1 = \frac{ds'}{ds} = \frac{\sqrt{\left(x_\varphi{}^2 + y_\varphi{}^2\right)d\varphi^2 + \left(x_\lambda{}^2 + y_\lambda{}^2\right)d\lambda^2 + 2\left(x_\varphi x_\lambda + y_\varphi y_\lambda\right)d\varphi d\lambda}}{\sqrt{\rho^2 d\varphi^2 + \nu^2 cos^2\varphi d\lambda^2}} \tag{5}$$

where $d\varphi$ and $d\lambda$ are the geographic coordinate differences between the infinitesimally close points so that $\varphi_j = \varphi_i + d\varphi$, $\lambda_j = \lambda_i + d\lambda$; x_φ, y_φ, x_λ and y_λ denote partial derivatives (evaluated all of them in point *i*) of the functions defining the map projection $x = x(\varphi, \lambda)$ and $y = y(\varphi, \lambda)$ respect to φ and λ; and ρ and ν are the principal radii of curvature of the ellipsoid (*R* for the case of a sphere). The linear distortion coefficients for the particular cases $d\lambda = 0$ (distortion along meridian) and $d\varphi = 0$ (distortion along parallel) are customary denoted by *h* and *k* respectively (Snyder, 1987). They can be easily computed as

$$h = k_{1\_meridian} = k_1(d\lambda = 0) = \frac{\sqrt{x_\varphi{}^2 + y_\varphi{}^2}}{\rho} \tag{6}$$

$$k = k_{1\_parallel} = k_1(d\varphi = 0) = \frac{\sqrt{x_\lambda{}^2 + y_\lambda{}^2}}{\nu cos\varphi} \tag{7}$$

It is well-known (Snyder, 1987) that in a conformal projection, given a point *i*, the linear distortion coefficient is independent of the direction *ij* (in contrast, for a non-conformal projection, length distortion is dependent on the coordinates of *i as well as* on the bearing from *i* to *j*).

Therefore, for a point *i* in a conformal projection we have $k_1 = h = k$ regardless of the situation of the nearby point *j* (the linear distortion coefficient is independent of direction). For a conformal projection it is also well-known (Snyder, 1987; Rajakovic and Lapaine, 2010) that the areal distortion coefficient k_2 – ratio of the projected differential area dS' to the original area on the ellipsoid or sphere dS – equals k_1 squared

$$k_2 = \frac{dS'}{dS} = k_1{}^2 \tag{8}$$

Other general measures of distortion include Tissot's ellipses (Snyder, 1987; Bauer-Marschallinger *et al.*, 2014) and derived measures (e.g. averaged ratio between complementary profiles, Yan *et al.*, 2016). However, for the case of a conformal projection (no angular distortion, linear distortion k_1, areal distortion $k_2 = k_1^2$ and Tissot's ellipses degenerated to circles of radius k_1) it seems sensible to study only k_1 and, in particular, its typical deviation from the optimum value 1, as we will see next.

Different optimization criteria have been proposed in the past, including the minimization of extreme linear distortions (Rajakovic and Lapaine, 2010) and minimization of several distortion estimators, such as the one introduced by Gilbert (1974) as

$$E_G = \frac{(s - s')^2}{\sqrt{s^2 s'^2}} \quad (9)$$

where *s* and *s'* are the original distance on the sphere or ellipsoid surface and the projected distance, respectively, to be obtained and averaged over a sufficiently large number of randomly selected pairs of points in order to obtain an overall estimator of the distortion for the projection.

By virtue of Eq. (5) we can write

$$s' = \int_0^s k_1 ds = k_1 s \quad (10)$$

where in the last equality we have denoted by k_1 the average linear distortion factor in the line (mean value theorem for integrals), so that substitution of Eq. (10) into Eq. (9) permits us to write

$$E_G = \frac{(s - k_1 s)^2}{\sqrt{s^2 k_1^2 s^2}} = \frac{(1 - k_1)^2}{k_1} \quad (11)$$

In the same fashion, Peters (1975) proposed the use of his estimator

$$E_P = \frac{|s - s'|}{|s + s'|} \quad (12)$$

which, again, using Eq. (10) we can transform (Canters, 2002) into

$$E_P = \frac{|1 - k_1|}{|1 + k_1|} \quad (13)$$

Other classic distortion estimators include the integral evaluation of Airy (1861) and Jordan (1896)'s measures, given respectively by

$$e_{A2} = \frac{1}{2}\left[(a_i - 1)^2 + (b_i - 1)^2\right] \quad (14)$$

being a_i and b_i the maximum and minimum linear distortion coefficients at the sample point, and

$$e_J = \frac{1}{2\pi}\int_0^{2\pi} (k_{1i} - 1)^2 d\alpha \quad (15)$$

For conformal projections ($a_i = b_i = k_{1i}$) these are respectively simplified to

$$e_{A2} = (k_{1i} - 1)^2 \quad (16)$$

and

$$e_J = (k_{1i} - 1)^2 \quad (17)$$

In practice the mean distortion value can be calculated by dividing the region into *n* smaller areas, determining the value for the midpoint of each and computing the average value (Canters, 2002).

This discrete evaluation can be interpreted as an approximation, depending on the number and distribution of the points, to the computation by using integrals .

We can therefore characterize the overall linear distortion of a projection by computing the squared differences of the linear distortion factor k_1 with respect to 1 – Airy and Jordan's measures for the case of conformal projections – for a given (large) set of n sample points, obtaining thus a typical measure for the distortion Δk_1 as

$$\Delta k_1 = \sqrt{\frac{1}{n}\sum_{i=1}^{n}(k_{1i}-1)^2} \tag{18}$$

The formula remembers that of the standard deviation only taking here 1 (the optimum value for k_1) instead of the average value of the sample. It will be referred to by the name of *typical distortion* and used as optimization function for the subsequent computations. It may be worth noting that a simple arithmetic mean of the differences of the linear distortion factor k_1 with respect to 1 might not give meaningful information about the possible distortions since large positive values could be cancelled out by large negative values and is therefore not recommended. For the case of weighted latitude-longitude lattices – weight according to Eq. (1) – the corresponding function to be used is

$$\Delta k_1 = \sqrt{\frac{\sum_{i=1}^{n}(w_i k_{1i}-1)^2}{\sum_{i=1}^{n} w_i}} \tag{19}$$

2.4. Optimization method

Map projections have some parameters (e.g. latitude of standard parallels) that have to be carefully selected in order to minimize the inevitable resulting distortions. The question of finding the best values for some parameters that yield the optimum value for a derived function is called an optimization problem. In general form, the optimization problem, i.e. the determination of the optimum vector $\boldsymbol{x}$ within a prescribed search domain D that makes the objective function f reach the global minimum, is formulated as

$$\begin{cases} \min \; f(\boldsymbol{x}) \\ \text{subject to } \; \boldsymbol{x} \in D \end{cases} \tag{20}$$

In our present case, the so-called objective function f will be Eq. (18) for some variables to optimize $\boldsymbol{x}$ (e.g. latitude of standard parallels) in the desired domain D (defined by some boundaries for the area of interest or, simply, the entire Earth).

One of the most successful methods devised for solving optimization problems is the Simulated Annealing (SA) method, originally developed by Metropolis et al. (1953), which emulates the process of crystalline network self-construction. It has been extensively used in the last years, particularly in the field of geosciences (e.g. Berné and Baselga, 2004; Santé-Riveira *et al.*, 2008; Baselga, 2011; Sharma, 2012; Chimi-Chiadjeu *et al.*, 2013; and Soltani-Mohammadi *et al.*, 2016). We will not delve into the many technicalities of the method and simply refer to specific publications (e.g. van Laarhoven and Aarts, 1987; Pardalos and Romeijn, 2002).

We will compare our results with alternative procedures for defining the latitudes of standard parallels in conic projections, in particular with the 1/6 rule of thumb consisting in placing the standard parallels at 1/6th of the maximum and minimum latitudes (e.g. Fenna, 2007; and Jenny,

2012) and the work by Savric and Jenny (2016), which gives polynomial models to determine standard parallels for three conic projections given the spatial extent of the desired mapped area.

3. Evaluation of map distortions

We analyze here the Lambert Conformal Conic projection that was first recommended by EuroGeographics (Annoni *et al.*, 2003) and then officially adopted by INSPIRE D2.8.I.1 (2014) as the standard for conformal mapping in Europe. This projection is also the same (including standard parallels) known as EPSG3034 in the database initially developed by the European Petroleum Survey Group – and currently maintained by the International Association of Oil & Gas Producers (OGP) – which has become a standard for the definition of coordinate reference systems (International Organization for Standardization, 2007).

This projection is to be used in Europe along with the official reference system ETRS89 with the defining parameters given in Table 1 (Annoni *et al.*, 2003).

Table 1
Defining parameters for Lambert Conformal Conic projection for Europe in ETRS89 system and bounding box as given in (Annoni *et al.*, 2003).

Parameter	Value
lower standard parallel latitude φ_l	35º N
upper standard parallel latitude φ_u	65º N
latitude of (false) grid origin φ_b	52º N
longitude of (false) grid origin λ_0	10º E
False northing N_0	2800000
False easting E_0	4000000
Maximum latitude φ_{max}	71º N
Minimum latitude φ_{min}	27º N
Maximum longitude λ_{max}	45º E
Minimum longitude λ_{min}	30º W

Defining *a* and *b* as the major and minor semiaxes of the ellipsoid (ellipsoid GRS80 for the case of reference system ETRS89), *f* ellipsoid flattening, and *e* its first eccentricity, we can subsequently compute for a point to be projected of latitude φ and longitude λ (Annoni *et al.*, 2003):

$$Q_l = \frac{1}{2}\left[\ln\left(\frac{1+\sin\varphi_l}{1-\sin\varphi_l}\right) - e\ln\left(\frac{1+e\sin\varphi_l}{1-e\sin\varphi_l}\right)\right] \quad (21)$$

$$W_l = \left(1-e^2\sin^2\varphi_l\right)^{1/2} \quad (22)$$

$$Q_u = \frac{1}{2}\left[\ln\left(\frac{1+\sin\varphi_u}{1-\sin\varphi_u}\right) - e\ln\left(\frac{1+e\sin\varphi_u}{1-e\sin\varphi_u}\right)\right] \quad (23)$$

$$W_u = \left(1-e^2\sin^2\varphi_u\right)^{1/2} \quad (24)$$

$$\sin\varphi_0 = \frac{\ln\left(\frac{W_u\cos\varphi_l}{W_l\cos\varphi_u}\right)}{Q_u - Q_l} \quad (25)$$

$$K = \frac{a\cos\varphi_l\exp\left(Q_l\sin\varphi_0\right)}{W_l\sin\varphi_0} \quad (26)$$

$$Q = \frac{1}{2}\left[\ln\left(\frac{1+\sin\varphi}{1-\sin\varphi}\right) - e\ln\left(\frac{1+e\sin\varphi}{1-e\sin\varphi}\right)\right] \tag{27}$$

$$R = \frac{K}{\exp(Q\sin\varphi_0)} \tag{28}$$

$$k = \left(1-e^2\sin^2\varphi\right)^{1/2}\frac{R\sin\varphi_0}{a\cos\varphi} \tag{29}$$

After computation of all the auxiliary quantities we arrive at the linear distortion coefficient k. (Note: remember the fact that $k_1 = h = k$ with Eqs. (5)-(7) since it is a conformal projection).

Now Annoni *et al.* (2003) give maximum and minimum linear distortion coefficients in the given boundaries, respectively 43704 ppm and -34378 ppm, but do not provide a figure for the *typical distortion* that could be expected. We will now use Eqs. (21)-(29) to evaluate the typical distortion – Eq. (18) – that is produced in this map projection for the assumed bounding box using different lattices (of latitude-longitude and Fibonacci types).

With the use of latitude-longitude lattices we find that we need a very large number of sampling points in the area (small step size δ) to obtain a value for Eq. (18) that is somewhat stable (i.e. that does not depend significantly on the number of sampling points), and even then the value keeps oscillating a bit.

When we use weighted latitude-longitude lattices we find more stable results and a significantly quicker convergence. However, both unweighted and weighted latitude-longitude lattices are clearly outperformed by the use of Fibonacci lattices, which yield a very quick and stable convergence to the final value $\Delta k_1 = 0.024687 = 24687\ \text{ppm}$ Table 2 and Fig. 3 summarize these results.

Table 2
Intervals of typical distortion values Δk_1 in terms of different number of lattice points in the area under study for three types of lattices: latitude-longitude, weighted latitude-longitude and Fibonacci.

Δk_1 value (ppm)	Lat-lon lattice: No. of points	Weighted lat-lon lattice: No. of points	Fibonacci lattice: No. of points
24687 ± 100 ppm	~300000	~83000	~430
24687 ± 10 ppm	-	~1000000	~6800
24687 ± 1 ppm	-	-	~27000

We stopped the computations when lattices reached a few million sampling points due to their high computational cost (several minutes in a standard personal computer) therefore some cases in the table could not even be computed. We can see that by using unweighted latitude-longitude lattices we have trouble to find a solution value that is stable to the level of 100 ppm. In Fig. 3 we can see that the main reason is that the estimate we get for Δk_1 is biased due to the unnecessary higher density of sampling points at higher latitudes. The computation is improved by the use of weighted latitude-longitude lattices, by which we can reach with effort a solution within 10 ppm. By contrast, the use of Fibonacci lattices permits us to obtain a quick convergence so that a solution within 1 ppm can easily be obtained by using around 27000 sampling points only.

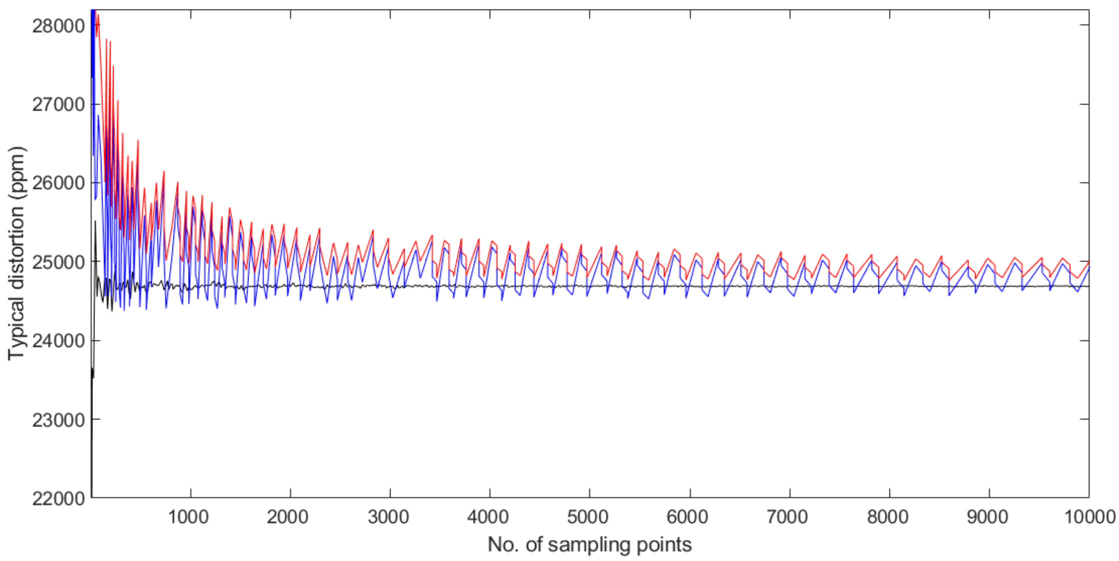

Fig. 3. Typical distortion values Δk_1 in terms of different number of lattice points (only up to 10000 points shown here) using three types of lattices: latitude-longitude (red), weighted latitude-longitude (blue) and Fibonacci (black).

We have shown that the typical distortion to be expected for the Lambert Conformal Conic projection using the parameters and bounding box defined for Europe, Table 1, is 24687 ppm and that it can be easily obtained with a small number of sampling points if we use a Fibonacci lattice

4. Optimization of map projections

We examine now whether the typical distortion value for the Lambert Conformal Conic projection can be improved by the use of different standard parallels than the ones conventionally used in Europe as well as compute the best ones for using the projection in Spain.

The following new procedure optimizes a map projection by computing the standard parallels that minimize the typical distortion of the desired area. We understand the question as a global optimization problem in which the typical distortion Δk_1 has to be minimized for a sufficient and efficient lattice of the area under study being the standard parallel latitudes the variables to optimize.

4.1. Optimization of Lambert Conformal Conic projection for Europe

We see now how the standard parallels included as the defining variables of the Lambert Conformal Conic projection for Europe, Table 1, can be optimized so that the typical distortion of the area, Eq. (18) using Eq. (29) as the particular linear distortion coefficient, can be minimized. We will use here the simulated annealing method as the optimization method (eventually the final results should be the same by means of other competent optimization method) and a Fibonacci lattice as efficient sampling set, once we have seen its excellent performance in the previous section.

We take into account the specific search domain, i.e. geographic boundaries in Table 1 (44º-wide in latitude and 75º-wide in longitude), use as the initial solution for the vector to optimize e.g. $\boldsymbol{x_0}$ = (φ_{l0}, φ_{u0}) = (35º, 65º), i.e. the values given in Table 1, and define the corresponding search domains as $\varphi_l \in [\varphi_{min}, (\varphi_{min}+\varphi_{max})/2]$ and $\varphi_u \in [(\varphi_{min}+\varphi_{max})/2, \varphi_{max.}]$. Given the results obtained in the previous section and wanting to have typical distortions computed to some 1 ppm, we decide to use a Fibonacci lattice with 28161 lattice points in the area. The algorithm converges to the optimum solution after some 100 to 150 iterations only (Figs. 4 and 5).

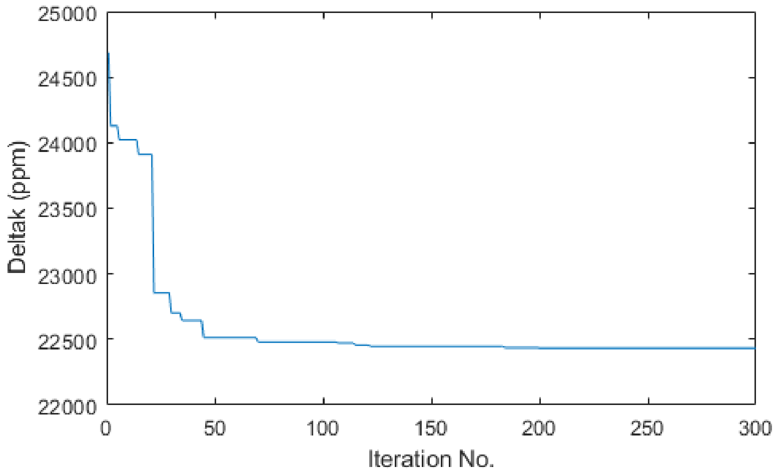

Fig. 4. Evolution of computed best value Δk_1 (ETRS89-Lambert Conformal Conic projection for Europe).

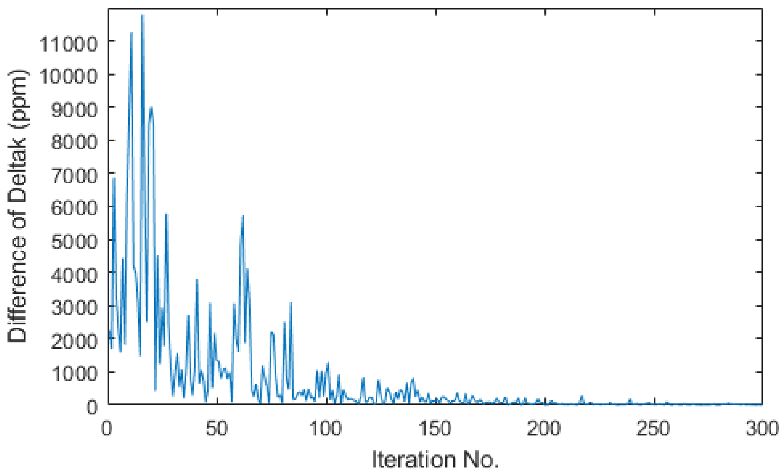

Fig. 5. Differences between current iteration value and final best value for Δk_1 (ETRS89-Lambert Conformal Conic projection for Europe).

We obtain a global optimum at φ_l = 36.06º, φ_u = 61.54º with Δk_1 = 22434 ppm. We obtain an almost indistinguishable result if we round to the next half-integer the standard parallel latitudes: φ_l = 36º, φ_u = 61.5º with Δk_1 = 22435 ppm.

These standard parallel latitudes are not very different from the ones customary used (φ_l = 35º, φ_u = 65º). However, we see a considerable decrease in the typical distortion of around 10% (from 24687 to 22435 ppm). In Table 3 we show the different results we obtain for the typical distortion Δk_1 also using the 1/6 rule of thumb and Savric and Jenny (2016) method. We also show other measures: Gilbert and Peters estimators, as well as average, maximum and minimum values of the linear distortion coefficient. It is worth mentioning that Savric and Jenny (2016)'s method was designed to optimize the standard parallels on the sphere, while we are using here ellipsoidal equations for the Lambert conformal conic projection. Savric and Jenny's method also assumes symmetry along the central meridian for the area of interest; therefore, we had to set symmetrical limits in longitude for the computation of optimum standard parallels with it, although the final evaluation of typical distortion was done for the non-symmetrical true area of interest.

Table 3
Different proposals for lower and upper standard parallels (φ_l and φ_u) along with their corresponding typical distortion (Δk_1), Gilbert and Peters estimators (E_G and E_P) and average, maximum and minimum values of linear distortion coefficient (k_{1avg}, k_{1max} and k_{1min}) for Lambert Conformal Conic projection for Europe.

Source	φ_l (º)	φ_u (º)	Δk_1 (ppm)	E_G (ppm)	E_P (ppm)	k_{1avg} (ppm)	k_{1max} (ppm)	k_{1min} (ppm)
INSPIRE D2.8.I.1 (2014) / Annoni et al.(2003) / EPSG3034	35	65	24687	617	11094	-9147	43704	-34378
1/6 rule of thumb (Jenny 2012, Fenna 2007)	34.33	63.67	23874	576	10673	-8518	54954	-32827
Savric and Jenny (2016)	37.55	58.68	23925	551	9064	7012	84836	-16988
Present method	36.06	61.54	22434	496	9514	-496	67600	-24733
Present method rounded to nearest half-integer	36	61.5	22435	496	9512	-566	68040	-24771

The standard parallels determined by our method clearly reduce the typical distortion in the area as compared with the parallels given by EuroGeographics and the INSPIRE directive (10% distortion reduction), 1/6 rule of thumb (6% distortion reduction), and Savric and Jenny (2016) polynomials (6% distortion reduction). Our method yields also the best solution in terms of Gilbert estimator and average distortion in the area, though it gives a second-best solution for Peters estimator just after Savric and Jenny's method, which, in turn, yields the highest distortion value in the area among all the different solutions. Having sought a solution that minimizes the typical distortion, Eq. (18), entailing minimization of Airy and Jordan estimators, we find a result that is also better than the alternative methods regarding Gilbert estimator and average distortion. It could be argued that our solution yields suboptimal values for other measures; however, considering that no single solution minimizes all values, the definition of the best projection in terms of the one minimizing the typical distortion as well as being the best in terms of other important distortion measures (average distortion and Gilbert estimator) seems a judicious one.

4.2. Optimization of Lambert Conformal Conic projection for Spain

We can use the same method to optimize the standard parallels to be used in the official Lambert Conformal Conic projection for Spain. A decree from the Gobierno del Estado Español (2007) commands that the ETRS89 reference system and the Lambert Conformal Conic projection be officially adopted for land representation at mapping scales of 1:500.000 or lower, without fixing, however, the particular latitudes to be used for the standard parallels. We use the same approach, simulated annealing as optimization method and a Fibonacci lattice for efficient sampling of the mapped area. As the problem geographic boundaries we use now those from EPSG3429 type area for "Spain mainland and Balearic Islands", namely φ_{min} = 35.26º N, φ_{max} = 43.82º N, λ_{min} = 9.37º W and λ_{max} = 4.39º E. We start with some arbitrary values in the search domain as initial solution e.g. $\boldsymbol{x_0} = (\varphi_{l0}, \varphi_{u0}) = (\varphi_{min}, \varphi_{max})$; the final solution being independent from this choice. The algorithm quickly converges to the optimum solution after a few iterations (Figs. 6 and 7).

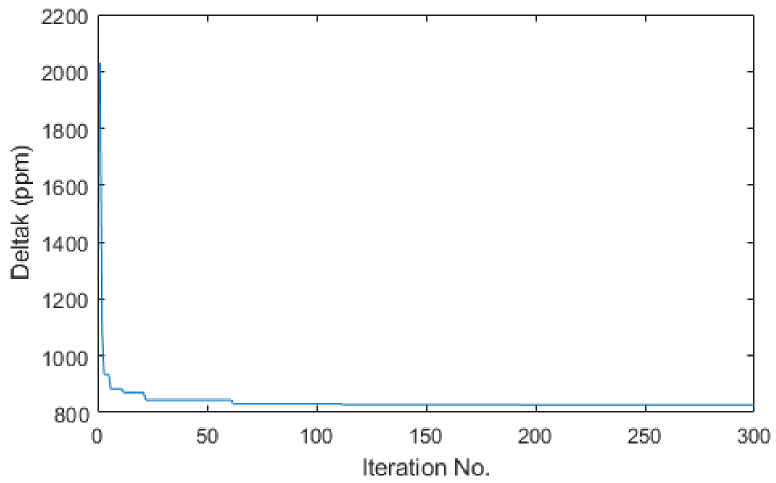

Fig. 6. Evolution of computed best value Δk_1 (ETRS89-Lambert Conformal Conic projection for Spain).

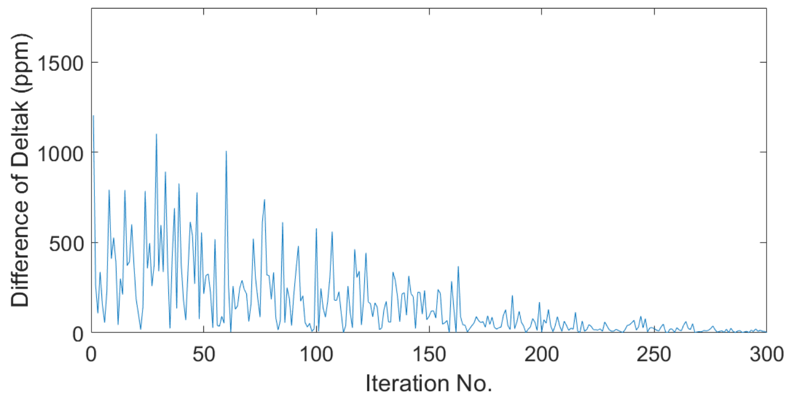

Fig. 7. Differences between current iteration value and final best value for Δk_1 (ETRS89-Lambert Conformal Conic projection for Spain).

We obtain a global optimum at φ_l = 37.07º, φ_u = 42.00º with Δk_1 = 827 ppm and a practically indistinguishable result if we round to the next integer these standard parallel latitudes: φ_l = 37º, φ_u = 42º with Δk_1 = 828 ppm.

We can see in Table 4 that there is a 1.5% distortion reduction for our proposal with respect to that of Savric and Jenny (2016) and a 7% distortion reduction with respect to that of the 1/6 rule of thumb. Similarly to the case of Europe (Table 3), our method gives also the best solution in terms of Gilbert estimator and average distortion in the area, and a second-best for Peters estimator right after Savric and Jenny's method, which, in turn, yields the highest distortion value in the area among all different solutions.

Table 4
Different proposals for lower and upper standard parallels (φ_l and φ_u) along with their corresponding typical distortions (Δk_1), Gilbert and Peters estimators (E_G and E_P) and average, maximum and minimum values of linear distortion coefficient (k_{1avg}, k_{1max} and k_{1min}) for Lambert Conformal Conic projection for Spain.

Source	φ_l (º)	φ_u (º)	Δk_1 (ppm)	E_G (ppm)	E_P (ppm)	k_{1avg} (ppm)	k_{1max} (ppm)	k_{1min} (ppm)
1/6 rule of thumb (Jenny 2012, Fenna 2007)	36.69	42.39	883	0.78	394	-311	1581	-1235
Savric and Jenny (2016)	37.29	41.82	840	0.70	348	145	2027	-779
Present method	37.07	42.00	827	0.68	356	2	1908	-922
Present method rounded to nearest integer	37	42	828	0.68	358	-25	1928	-948

5. Conclusions

In the present paper we have shown the clear advantages in performance of Fibonacci lattices with respect to the standards latitude-longitude lattices for numerical evaluation of map distortions.

We have computed the typical distortion for the Lambert Conformal Conic projection with their currently defined parameters and geographic boundaries for Europe, adopted as standard by INSPIRE, resulting in 24687 ppm. Further, we have optimized the defining parameters of this projection so that the typical distortion for the area of interest (Europe) is reduced a 10%. We therefore recommend a change in the definition of standard parallel latitudes for the Lambert Conformal Conic projection in Europe so that lower and upper standard parallels be set to 36º and 61.5º, respectively.

We also apply the optimization procedure to the determination of the best standard parallels for using the Lambert Conformal Conic projection in Spain, whose values remained unspecified by the National decree that commanded its official adoption. We obtain a best pair of standard parallels of latitudes 37º and 42º for which the typical distortion results in 828 ppm.

Acknowledgements

The author sincerely appreciates the comments, suggestions and computation double checking by the anonymous reviewers that helped improve the manuscript.

References

Airy, G. B., 1861. Explanation of a projection by balance of errors for maps applying to a very large extent of the Earth's surface, and comparison of this projection with other projections. London, Edimburgh and Dublin Philosophical Magazine, 4th ser., 22: 409–421.

Annoni, A., Luzet, C., Gubler, E. and Ihde, J., 2003. Map Projections for Europe. European Commission Joint Research Centre, Ispra, Italy. EUR 20120 EN.

Baselga, S., 2011. Second Order Design of Geodetic Networks by the Simulated Annealing Method. Journal of Surveying Engineering, 137(4): 167–173.

Baselga, S., 2014. Fundamentos de Cartografía Matemática. 2nd ed. Universitat Politècnica de València, València.

Bauer-Marschallinger, B., Sabel, D. and Wagner, W., 2014. Optimisation of global grids for high-resolution remote sensing data. Computers & Geosciences, 72: 84–93.

Berné, J.L. and Baselga, S., 2004. First-Order Design of Geodetic Networks using the Simulated Annealing Method. Journal of Geodesy, 78(1): 47–54.

Canters, F., 2002. Small-scale Map Projection Design. Taylor & Francis, London,

Canters, F., and Decleir, H., 1989. The World in Perspective: A Directory of World Map Projections. John Wiley and Sons, Chichester.

Chimi-Chiadjeu, O., Vannier, E., Dusséaux, R., Le Hégarat-Mascle, S. and Taconet, O., 2013. Using simulated annealing algorithm to move clod boundaries on seedbed digital elevation model. Computers & Geosciences, 57: 68–76.

Conway, J. H. and Sloane, N. J. A., 1998. Sphere packings, lattices and groups. 3rd edn. Springer, New York.

Crăciun, C., 2014. Homogeneity and EPR metrics for assessment of regular grids used in CW EPR powder simulations. Journal of Magnetic Resonance, 245: 63–78.

Fenna, D., 2007. Cartographic Science: A Compendium of Map Projections, with Derivations. CRC Press, Taylor & Francis Group, Boca Raton.

Gilbert, E. N,, 1974. Distortion in maps. Society for Industrial and Applied Mathematics Review, 16: 47–62.

Gobierno del Estado Español, 2007. Gobierno del Estado Español, Real Decreto 1071/2007, de 27 de julio, por el que se regula el sistema geodésico de referencia oficial en España. Boletín Oficial del Estado, 207: 35986–35989.

González, A., 2010. Measurement of Areas on a Sphere Using Fibonacci and Latitude–Longitude Lattices. Mathematical Geosciences, 42: 49–64.

INSPIRE D2.8.I.1, 2014. Data Specification on Coordinate Reference Systems – Technical Guidelines

International Organization for Standardization, 2007. Geographic information – Spatial referencing by coordinates (ISO Standard No. 19111). Retrieved from https://www.iso.org/standard/41126.html

Jenny, B., 2012. Adaptive composite map projections. IEEE Trans. Vis. Comput. Graph., 18(12): 2575–2582.

Jordan, W., 1896. Der mittlere Verzerrungsfehler. Zeitschrift für Vermessungswesen, 25: 249–252.

Koshy, T., 2001. Fibonacci and Lucas Numbers with Applications. Wiley-Interscience, New York.

Marques, R., Bouville, C., Ribardiere, M., Santos, L. P. and Bouatouch, K., 2013. Spherical Fibonacci Point Sets for Illumination Integrals. Computer Graphics Forum, 32(8): 134–143.

Metropolis, N., Rosenbluth, M., Rosenbluth, A., Teller, A., and Teller, E., 1953. Equation of state calculations by fast computing machines. J. Chem. Phys., 21(6): 1087–1092.

Monechi, B., Servedio, V. D. P. and Loreto, V., 2015. Congestion Transition in Air Traffic Networks. PLoS ONE, 10(5): e0125546. doi:10.1371/journal.pone.0125546

Pardalos, P. M., and Romeijn, H. E., eds., 2002. Handbook of global optimization, Vol 1&2, Kluwer Academic, Dordretch.

Peters, A. B., 1975. Wie man unsere Weltkarten der Erde ähnlicher machen kann. Kartographische Nachrichten, 25: 173–183.

Purser, R. J., 1999. Non-standard Grids. Proceedings of the ECMWF Seminar on Recent Developments in Numerical Methods for Atmospheric Modelling, p. 44-72, 7–11 September 1998.

Rajakovic, M., and Lapaine, M., 2010. The Best Conic Conformal Map Projection for the Territory of Croatia. Kartografija i Geoinformacije, 9(14): 24–44.

Santé-Riveira, I., Boullón-Magán, M., Crecente-Maseda, R. and Miranda-Barrós, D., 2008. Algorithm based on simulated annealing for land-use allocation. Computers & Geosciences, 34: 259–268.

Šavrič, B. and Jenny, B., 2016. Automating the selection of standard parallels for conic map projections. Comput. Geosci. 90: 202–212.

Sharma, S. P., 2012. VFSARES—a very fast simulated annealing FORTRAN program for interpretation of 1-D DC resistivity sounding data from various electrode arrays. Computers & Geosciences, 42: 177–188.

Snyder, J. P., 1987. Map Projections: A Working Manual. US Geological Survey, Washington, DC.

Soltani-Mohammadi, S., Safa, M. and Mokhtari, H., 2016. Comparison of particle swarm optimization and simulated annealing for locating additional boreholes considering combined variance minimization. Computers & Geosciences, 95: 146–155.

Sparrow, K. H. and Mercer, A. E., 2016. Predictability of US tornado outbreak seasons using ENSO and northern hemisphere geopotential height variability. Geoscience Frontiers, 7(1): 21–31.

Swinbank, R. and Purser, R. J., 2006. Fibonacci grids: A novel approach to global modelling. Quarterly Journal of the Royal Meteorological Society, 132: 1769–1793.

van Laarhoven, P. J. M. and Aarts, E. H. L., 1987. Simulated annealing: theory and applications, Reidel, Dordretch.

Yan, J., Song, X., Gong, G., 2016. Averaged ratio between complementary profiles for evaluating shape distortions of map projections and spherical hierarchical tessellations. Computers & Geosciences, 87: 41–55.